

Photodegradation of the algal toxin domoic acid in natural water matrices

René-Christian Bouillon,¹ Tika L. Knierim, Robert J. Kieber, Stephen A. Skrabal, and Jeffrey L. C. Wright

University of North Carolina, Wilmington, Department of Chemistry and Biochemistry, Wilmington, North Carolina, 28403

Abstract

We investigated the photodegradation rate of the powerful marine toxin domoic acid in a variety of natural water matrices. The observed first-order photodegradation rate coefficient (k_{obs}), obtained by linear regression of the logarithmic-transformed domoic acid concentrations versus irradiation time in simulated sunlight, was $0.15 \pm 0.01 \text{ h}^{-1}$ in coastal seawater. Photodegradation rate coefficients in deionized water were not significantly different than those in coastal seawater, indicating that domoic acid is mainly photodegraded through a direct photochemical pathway. Addition of 100 nmol L^{-1} spikes of iron III [Fe(III)] and copper II [Cu(II)] had no significant effect on domoic acid photodegradation, indicating that the formation of trace-metal chelates did not enhance photodegradation of the toxin in seawater. We observed an increase of domoic acid photodegradation rates with temperature with a corresponding energy of activation of 13 kJ mol^{-1} . The effect on photodegradation of pH, added humic material, and dissolved oxygen removal was also investigated. The quantum yield of domoic acid photodegradation in seawater decreased with increasing wavelength and decreasing energy of incoming radiation, with the average value ranging from 0.03 to 0.20 in the ultraviolet wavelength range (280–400 nm). Using these quantum yields together with modeled solar spectral irradiance and seawater optical properties, we estimated turnover rate coefficients for the photochemical degradation of domoic acid ranging from 0.017 to 0.035 d^{-1} . These observations indicate that sunlight-mediated reactions are an important, yet previously unrecognized, sink of dissolved domoic acid in seawater.

Domoic acid is a potent marine neurotoxin produced by *Pseudo-nitzschia* species. It is remarkably pervasive in North American coastal waters, where it is a threat to public health and some marine life and has resulted in severe economic losses in the shellfish and crustacean harvesting industry. Originally discovered as the causative agent in an episode of fatal human poisoning in eastern Canada in 1987 (Wright et al. 1989; Todd 1993), domoic acid was eventually linked to other epizootics, particularly on the western coast of North America (Horner et al. 1997), where it has resulted in the death of seabirds and mammals (Scholin et al. 2000; Lefebvre et al. 2002). The production and release of this water-soluble toxin has recently been proposed to have ecological roles for *Pseudo-nitzschia*, including the sequestration of iron III [Fe(III)] from Fe-depleted waters and the complexation of potentially toxic metal ions such as copper II [Cu(II)] (Rue and Bruland 2001; Maldonado et al. 2002).

Despite the significance of domoic acid to the biogeochemistry of aquatic systems, little is known regarding the fate of the toxin once it is released into the water column. This is a particularly significant question during bloom events, as the majority of toxin produced may not be transferred to higher trophic levels but may instead be released into the water column, where seawater extracellular concen-

trations can reach $>100 \text{ nmol L}^{-1}$, with cell concentrations of $>10^6 \text{ cells L}^{-1}$ (Doucette et al. 2002).

Microbial degradation of extracellular domoic acid is a likely fate of the toxin. Stewart et al. (1998) tested the ability of a variety of bacteria isolated from the marine environment and other marine organisms for their ability to biodegrade domoic acid. Interestingly, only a few bacteria isolated from certain shellfish tissues (e.g., *Mytilus edulis* and *Mya arenaria*) appeared to biodegrade domoic acid (Stewart et al. 1998). Those results indicate that biodegradation of extracellular domoic acid may not be the dominant elimination pathway of the toxin in seawater.

Another potentially important sink of dissolved domoic acid in seawater involves photochemical transformations. Domoic acid is a tricarboxylic amino acid related structurally to glutamic acid (Fig. 1). However, the toxin also possesses a side chain containing a conjugated double-bond moiety and a hind carboxylic group. It has been shown that the geometry of the double bonds in the side chain is related to the potency of the toxin (Hampson et al. 1992). Over the past 40 yr, many studies of unsaturated compounds similar to domoic acid have demonstrated the importance of photochemical *cis-trans* isomerization (Hammond et al. 1964; Zepp et al. 1985), in which the isomerizations occur through both direct and sensitized photochemical pathways (Turro 1978). Preliminary studies by Wright et al. (1990) have shown that similar photochemical processes may also be important for dissolved domoic acid. The authors found that exposure of elevated concentrations of domoic acid to high-energy ultraviolet radiation (253.7 nm) resulted in rapid photodegradation of the toxin in seawater. In a similar preliminary study, Bates et al. (2003) also demonstrated that relatively high concentrations of domoic acid are photode-

¹ Corresponding author (bouillonr@uncw.edu).

Acknowledgments

We thank Richard Lancaster and Monica Lassiter for technical support and Cédric Fichot for providing us with modeled attenuation coefficient. The constructive criticism provided by two anonymous reviewers on an earlier version of this manuscript are gratefully acknowledged. This research was supported by a grant from the National Science Foundation (OCE0326685).

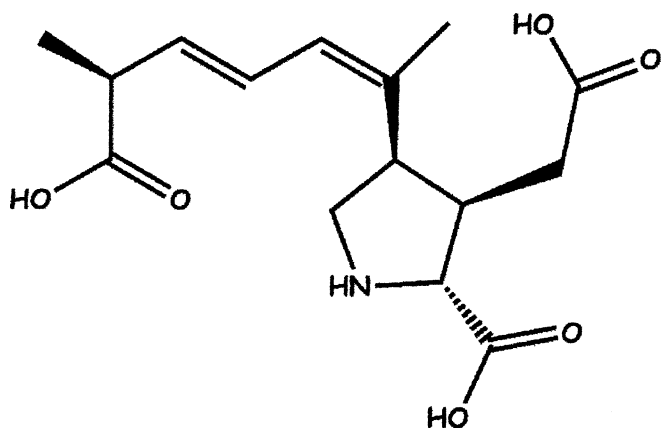


Fig. 1. Molecular structure of domoic acid in its neutral form.

graded upon exposure to simulated sunlight in coastal seawater (>290 nm).

Rue and Bruland (2001) recently demonstrated that domoic acid is an effective chelator for Cu(II) and Fe(III), both of which are bioactive trace metals of vital importance to a variety of biochemical processes occurring in natural waters. Both Fe and Cu undergo a variety of light-mediated redox reactions [involving Fe(II)/Fe(III) and Cu(I)/Cu(II) transformations] when complexed to organic ligands (Voelker et al. 2000; Barbeau et al. 2001). Therefore, the occurrence of the chelated domoic acid complexes may be important to the ultimate fate of the toxin in natural waters. It is hypothesized that photochemical degradation and trace-metal complexation are thus important factors controlling the biogeochemical cycling and ultimate fate of domoic acid in natural waters.

The aim of this work was to carry out the first detailed kinetic study of the photodegradation rate of extracellular domoic acid in order to quantify the importance of this removal process in coastal seawater. Two kinds of irradiation experiments were carried out: full spectral irradiation and monochromatic irradiation experiments. The purpose of the full spectral irradiation experiments was to quantify the photodegradation rate of domoic acid in seawater under environmentally relevant conditions. The potential importance of a variety of environmental factors, such as trace metal complexation, is also discussed. Monochromatic irradiation experiments were performed to determine the wavelength dependence of photodegradation of domoic acid. To our knowledge, this is the first time the wavelength dependence of the photochemical transformation of any algal toxin has been determined. Finally, the potential in situ loss rates and turnover rate constants for domoic acid photodegradation were modeled for various coastal locations. This information can ultimately be used to assess the biogeochemical cycling of the extracellular fraction of the toxin in seawater.

Materials and methods

Seawater sample collection and irradiation solution details—Solutions for photochemical experiments were prepared using both deionized water (DIW) and coastal sea-

water. DIW ($18 \text{ M}\Omega \text{ cm}^{-1}$) was supplied from a Millipore water purification system (Millipore). Natural Wrightsville Beach seawater samples (WBSW) were collected in 10-liter fluorinated polyethylene carboys from Wrightsville Beach, North Carolina (34.2°N , 77.8°W). Seawater samples were filtered through a Meissner Stylux $0.2\text{-}\mu\text{m}$ (500-cm^2) filter capsule pre-rinsed with a copious amount of seawater. Prior to sample collection, filter capsules were pre-cleaned with acidic solution (pH 2, Fisher TraceMetal grade HCl) followed by DIW. Seawater samples were stored in the dark at 5°C .

Water samples were enriched with domoic acid by addition of a $32.2\text{-}\mu\text{mol L}^{-1}$ aqueous domoic acid (95%, MP Biomedicals) stock solution to yield environmentally relevant final concentrations. Stock solutions of domoic acid were prepared by dissolving 2.5 mg of domoic acid into 250 mL of an aqueous solution of acetonitrile (10%). In order to limit domoic acid bacterial decomposition, acetonitrile was used as a photochemically inert co-solvent (Lemaire et al. 1982). High-performance liquid chromatography-ultraviolet (HPLC-UV) analysis (242 nm) of the domoic acid stock solution indicated that there were no other absorbing compounds present in the solution.

A description of each irradiation solution used in this study is presented in Table 1. The number of replicates and initial concentration (or range) for each treatment is indicated in Table 1. Measurements of pH were carried out with an Orion Ross 8102 combination electrode calibrated using NIST buffers. In order to determine whether domoic acid is degraded through a direct photochemical pathway, an experiment was performed using DIW (pH 5.1) spiked with domoic acid stock solution. The series of six experiments ($n = 6$) referred to in Table 1 as WBSW were prepared by spiking water collected from Wrightsville Beach with domoic acid stock solution. Another experiment was performed in which humic acid material was added to a domoic acid sample prepared with deionized water (DIW+HUM). Humic acid materials were extracted from the Cape Fear River, North Carolina, as described in Shank et al. (2004b). Extracted humic acid was added to the irradiation solution to yield a final concentration of $\sim 20 \text{ mg L}^{-1}$, which is somewhat higher than concentrations found in coastal oceanic waters.

Iron(III) and Cu(II) were added to domoic acid solutions to determine the effect of trace-metal complexation of domoic acid on its photodegradation rate. In preparation for these trace-metal experiments, all implements, including quartz cells and pipette tips, were soaked in 10% HCl for 24 h, rinsed with deionized water, and dried in a class 100 laminar flow clean bench. A secondary stock aqueous solution of Fe(III) was prepared by adding $500 \mu\text{L}$ of $1,000 \text{ mg L}^{-1}$ ferric nitrate standard (Fisher) to 4.5 mL DIW. The secondary Fe(III) stock solution was spiked to both deionized water (DIW+Fe) and Wrightsville Beach seawater (WBSW+Fe) containing domoic acid to yield a final Fe concentration of 107 nmol L^{-1} . WBSW+Fe experiments were performed four times ($n = 4$) at an ambient pH of 8. In addition, a series of experiments (WBSW+Fe-pH4; WBSW+Fe-pH5; WBSW+Fe-pH6; and WBSW+Fe-pH7) were conducted in order to determine the effect of pH on

Table 1. Experimental conditions and observed first-order rate coefficients of domoic acid photodegradation (k_{obs}) for each experiment under simulated sunlight. n represents the number of times each photodegradation experiment was repeated, with its corresponding standard deviation.*

Experiment	Temperature (°C)	pH	Initial domoic acid concentration (nmol L ⁻¹)	k_{obs} (h ⁻¹)
WBSW	23±1	8.1	84.0–256	0.15±0.01 ($n=6$)
DIW	23±1	5.1	325	0.16 ($n=1$)
DIW+HUM	23±1	6.0	325	0.15 ($n=1$)
DIW+Fe	23±1	4.8	93.5	0.26 ($n=1$)
WBSW+Fe	23±1	8.1	73.1–82.0	0.14±0.01 ($n=4$)
WBSW+Fe-pH4	23±1	4.1	84.7	0.17 ($n=1$)
WBSW+Fe-pH5	23±1	5.3	90.3	0.16 ($n=1$)
WBSW+Fe-pH6	23±1	6.5	74.4	0.14 ($n=1$)
WBSW+Fe-pH7	23±1	7.2	81.1	0.15 ($n=1$)
WBSW+Cu	23±1	8.1	72.9–84.4	0.15±0.01 ($n=4$)
WBSW-no-O ₂	23±1	8.4	82.8	0.15 ($n=1$)
WBSW-UV-TMC	23±1	6.5	85.5	0.15 ($n=1$)
WBSW	5±1	8.0	94.1	0.12 ($n=1$)
WBSW	10±1	8.1	91.5	0.13 ($n=1$)
WBSW	15±1	8.2	92.4	0.15 ($n=1$)
WBSW	20±1	8.1	86.3	0.15 ($n=1$)

* WBSW, Wrightsville Beach seawater; DIW, Milli-Q deionized water; HUM, humic substances; UV-TMC, UV treated, trace-metal clean.

the photodegradation of domoic acid in WBSW spiked with 107 nmol L⁻¹ Fe(III). The pH of irradiation solutions was then adjusted to 4, 5, 6, or 7 with high-purity HCl (Fisher Optima). A 20.0- μ mol L⁻¹ cupric nitrate standard solution (EMD Chemical) was added to a domoic acid WBSW solution to yield a final concentration of approximately 100 nmol L⁻¹ Cu(II) (WBSW+Cu). WBSW+Cu experiments were performed four times ($n = 4$). The pH of the Cu(II)-domoic acid solution was then adjusted to \sim 8.0 by adding high-purity NH₄OH (Fisher Optima). The Fe(III)-domoic acid and Cu(II)-domoic acid solutions were allowed to equilibrate overnight in the dark at room temperature before use to allow for metal complexation to the toxin.

The role of oxygen in the photochemical degradation of domoic acid was investigated by removal of oxygen prior to irradiation. A domoic acid stock solution was added to a WBSW sample similar to the earlier irradiation experiments discussed above; however, in this case, the sample was placed in a glove bag filled with N₂, bubbled for 4 h with N₂, and allowed to incubate overnight in the dark under N₂ before use. The N₂-purged solution (WBSW-no-O₂) was then distributed into the irradiation quartz cells, and the cells were capped inside the glove bag.

Irradiation system and exposure details—Full spectral irradiation experiments were performed using a Spectral Energy solar simulator (LH 153 lamp housing, 1,000-W Xe lamp, LPS 256 SM power supply). The solar simulator was equipped with a sun lens diffuser and an AM1 filter that eliminates unwanted wavelengths not found in the solar spectrum (<280 nm). Irradiance measurements inside the solar simulator were made with an Ocean Optics SD2000 spectrophotometer connected to a fiber optic cable terminated with a CC-UV cosine collector. The system was calibrated with a NIST traceable tungsten lamp, and data were collected with OOIrradTM software. Irradiance was measured

at the beginning and end of each photochemical experiment. Irradiation solutions were distributed in eleven 10-cm-long (\sim 30-mL) spectrophotometric quartz cells. Ten cells were vertically positioned, with the flat part of the cells exposed to irradiance, within a circular carrier immersed into a water-thermostated bath. The cell holder was rotated 90° every half hour in order to ensure that all cells received the same radiation intensity. Unless otherwise noted, the temperature during the experiments was 23°C \pm 1°C. An 11th cell was placed in a dark incubation chamber at the same temperature to serve as a dark control. The irradiation solutions were exposed to simulated sunlight for a total of 10 h. Two quartz cells were removed from the solar simulator for domoic acid determination every 2 h, with the concentration of domoic acid determined in each cell. Duplicate 400- μ L aliquots were removed from the dark control (the 11th cell) every 2 h for domoic acid determination. The initial concentration of domoic acid was determined by removing duplicate 400- μ L aliquots from the dark control. Observed first-order rate coefficients of domoic acid photodegradation in samples, k_{obs} , were obtained by linear regression of the logarithmic-transformed domoic acid concentrations versus irradiation time and were normalized and corrected as necessary (*see Results and discussion*). Statistical comparison of k_{obs} for different treatments was performed using a Student's t -test for the comparison of two slopes (Zar 1984) at the 95% confidence level.

Wavelength-dependent quantum yields for domoic acid photodegradation were performed with a Spectral Energy monochromatic irradiation system (LH 153 lamp housing, 1,000-W Hg-Xe lamp, LPS 256 SM power supply) equipped with a GM 252-20 high-intensity 0.25-m grating monochromator. Bandwidths of 10 nm centered at 280.0, 290.0, 300.0, 313.0, 334.1, 366.0, and 404.5 nm were used in this study. Irradiation times for each selected waveband can be found in Table 2. An AM1 filter was used for waveband 404.5 to

Table 2. Quantum yield for domoic acid photodegradation [$\Phi_{DA}(\lambda)$] in deionized water (DIW) and in Wrightsville Beach seawater (WBSW). n represents the number of times each photodegradation experiment was repeated, with its corresponding standard deviation. The temperature during experiments was $23^\circ\text{C} \pm 1^\circ\text{C}$.

Wavelength (nm)	Irradiation time (h)	DIW		WBSW	
		Initial domoic acid concentration (nmol L ⁻¹)	$\Phi_{DA}(\lambda)$	Initial domoic acid concentration (nmol L ⁻¹)	$\Phi_{DA}(\lambda)$
280.0	18	78.8–86.3	0.200 ± 0.014 ($n=3$)	89.2–122	0.163 ± 0.006 ($n=3$)
290.0	18	78.2–79.8	0.138 ± 0.011 ($n=3$)	89.7–121	0.136 ± 0.004 ($n=3$)
300.0	18	68.2–72.5	0.056 ± 0.006 ($n=3$)	89.0–133	0.056 ± 0.004 ($n=3$)
313.0	24	76.2–76.5	0.036 ± 0.005 ($n=3$)	120–133	0.036 ± 0.005 ($n=3$)
334.1	72	73.3–88.0	0.066 ± 0.001 ($n=3$)	111–130	0.043 ± 0.003 ($n=3$)
366.0	72	71.5–135	0.037 ± 0.005 ($n=3$)	111–124	0.032 ± 0.004 ($n=3$)
404.5	96	136–140	0.0 ± 0 ($n=3$)	105–110	0.0 ± 0 ($n=3$)

minimize effects of second-order irradiance. Irradiance was measured using an International Light research radiometer model IL1700 (5-V bias off) with a SED033 detector, calibrated using a conventional potassium ferrioxalate actinometer (Hatchard and Parker 1956). Water samples were irradiated in 10-cm-long (~ 30 -mL), spectrophotometric quartz cells for the length of time sufficient to bring about 50% loss of domoic acid initial concentration. Irradiation solutions were kept at room temperature ($23^\circ\text{C} \pm 1^\circ\text{C}$). Monochromatic irradiation experiments were performed in triplicate for each selected waveband. For each irradiation solution, the concentration of domoic acid was determined in triplicate.

Domoic acid determination—The concentration of dissolved domoic acid was determined using a modified version of the fluorenylmethoxycarbonyl (FMOC)–HPLC method described by Pocklington et al. (1990). This method is based on fluorometric detection after a precolumn reaction to produce fluorescent derivatives separable by HPLC. Chromatography was performed using a reversed-phase C_{18} column (4.6-mm inner diameter \times 25-cm packed with 5 μm C_{18} bonded silica gel; Vydac 201TP column) at a column temperature of 55°C . A Hewlett-Packard 1100 system equipped with a quaternary gradient pump coupled to an external Shimadzu PF-55I PC spectrofluorometric detector was used with an injection volume of 10 μL . Analyses conditions are described in detail by Wright and Quilliam (1995). Mobile phase (1 mL min⁻¹) consisted of deionized water (A) and acetonitrile (B) in a binary system, with 0.1% trifluoroacetic acid as an additive. The elution gradient was from 30% to 70% B over 15 min, followed by an increase to 100% B over 2 min, which was maintained for 5 min, then returned to initial conditions at 27 min and held for 8 min before the next injection. The detection limit, defined as a signal to noise ratio of 3, was 5 nmol L⁻¹, with a relative standard deviation of approximately 1% at typical seawater concentrations. The chromatographic conditions resulted in the separation of domoic acid from its geometrical isomers, as described by Wright et al. (1990). The certified calibration solutions of domoic acid (99.5 mg L⁻¹) were purchased through the National Research Council of Canada Reference Materials Program. HPLC-FMOC determination of the cer-

tified calibration solutions indicated that the solution of domoic acid was geometrically pure (data not shown).

Absorbance measurements—Absorbance measurements were carried out using a Varian CARY3 dual-beam scanning spectrophotometer at 1-nm resolution zeroed against DIW. The domoic acid solution and DIW for the blank were equilibrated at room temperature prior to absorbance determination. The molar absorption coefficient of domoic acid from 190 to 500 nm was determined in DIW at pH 5.1. A domoic acid concentration of 6.0 $\mu\text{mol L}^{-1}$ was used for absorption measurements made below 280 nm. The domoic acid concentration was increased to 302 $\mu\text{mol L}^{-1}$ to acquire absorption spectra at longer wavelengths, thus allowing for more accurate determination of the absorbance. The molar absorption coefficient of domoic acid was determined using Beer's Law.

Modeling studies—In order to evaluate the relative importance of photochemical processes as an elimination mechanism for domoic acid in natural waters, environmental turnover rate coefficients for domoic acid photodegradation were estimated using modeled solar irradiance and seawater attenuation coefficients for a concentration of domoic acid of 100 nmol L⁻¹. Three different locations were chosen: Monterey Bay, California (36.788°N, 122.053°W; 21 September 2004), Washington State Coast (48.169°N, 125.525°W; 01 October 2004), and coastal Prince Edward Island (46.597°N, 63.795°W; 2 October 2004). Environmental photochemical rates and rate constants have been computed for these hypothetical dates, since domoic acid-producing algae frequently bloom during late summer/early fall at each of these locations (Bates et al. 1989; Trainer et al. 2000; Trainer et al. 2002).

The TUV model developed by Madronich and Flocke (1998) was used to simulate solar spectral irradiance reaching the water surface [$E_d(\lambda, 0+)$] as a function of latitude, time, total ozone, and other atmospheric parameters. The downwelling spectral irradiance just below the sea surface $E_d(\lambda, 0-)$ (mol photons m⁻² d⁻¹ nm⁻¹) was computed using the percentage irradiance loss by reflection at the sea-air interface as a function of solar elevation (Jerlov 1976). $E_d(\lambda, 0-)$ was converted to downwelling scalar irradiance $E_o(\lambda,$

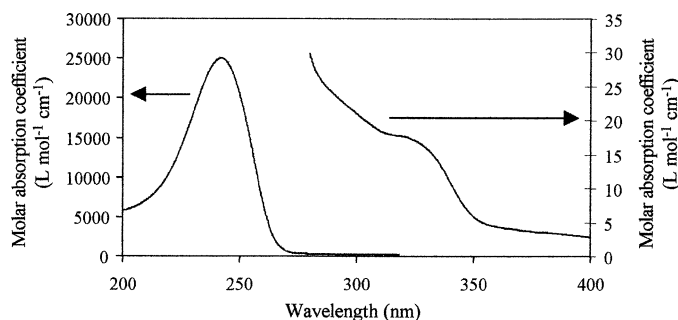


Fig. 2. Absorption spectrum of domoic acid in deionized water at pH 5.1 (note the different scales).

0–), assuming that upwelling irradiance was negligible, using the relation

$$E_o(\lambda, 0-) \approx E_d(\lambda, 0-)/\bar{\mu}_d \quad (1)$$

where $\bar{\mu}_d$ (dimensionless) is the average cosine of the downwelling irradiance. The value of $\bar{\mu}_d$ was estimated using

$$\bar{\mu}_d^{-1} = f_{\text{dir}}(\lambda)\sec \theta + 1.2f_{\text{diff}}(\lambda) \quad (2)$$

where $f_{\text{dir}}(\lambda)$ and $f_{\text{diff}}(\lambda)$ are the fractions of solar irradiance direct and diffuse, respectively, and θ is the angle of refraction of the direct component of solar irradiance reaching the water surface (Zepp and Cline 1977; Gordon 1989).

The modeled surface downwelling irradiance was then propagated through the water column using the spectral attenuation coefficients for downwelling irradiance [$K_d(\lambda)$: m^{-1}]. The spectral downwelling irradiance $E_o(\lambda, z)$ at each depth (1-m intervals), for wavelengths at 1-nm intervals ranging from 280 to 400 nm, was calculated using Beer's Law (Kirk 1994):

$$E_o(\lambda, z) = E_o(\lambda, 0-)e^{-K_d(\lambda)z} \quad (3)$$

Based on an approach proposed by Cullen et al. (1997), $K_d(\lambda)$ values were modeled using the algorithm *SeaUV_C*, developed by C. Fichot (University of Georgia at Athens), that relates remote sensing reflectance to in situ $K_d(\lambda)$. Briefly, the algorithm has been obtained by performing a principal component analysis on remote sensing reflectance data to define four new orthogonal dimensions of ocean color, which were used as predictors in multiple linear regressions of $K_d(\lambda)$ (Fichot 2004). The *SeaUV_C* algorithm was applied to remote sensing reflectance obtained from *SeaWiFS* archive data scenes for 21 September 2004 (Monterey Bay), 1 October 2004 (Washington State Coast), and 2 October 2004 (Prince Edward Island) to predict $K_d(\lambda)$ at 320, 340, 380, 412, 443, and 490 nm. Predicted $K_d(\lambda)$ values were fitted with a single exponential to estimate $K_d(\lambda)$ from 280 to 400 nm.

Results and discussion

Molar absorption coefficients—Molar absorption coefficients of domoic acid were determined from 190 to 500 nm in DIW at pH 5.1 (Fig. 2). In the wavelength range from 190 to 500 nm, domoic acid absorbs with a peak centered between 200 and 275 nm, with a maximum absorption (ϵ_{max})

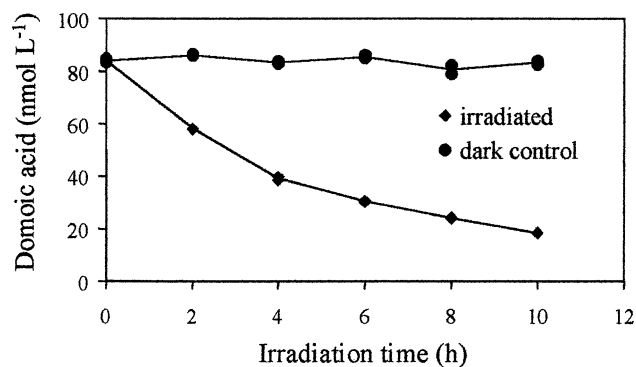


Fig. 3. Concentration of domoic acid (nmol L^{-1}) in simulated sunlight exposed and dark control samples as a function of irradiation time (h) in Wrightsville Beach Seawater (WBSW). Salinity 34; pH 8.1.

of $26,100 \text{ L mol}^{-1} \text{ cm}^{-1}$ at 242 nm. The wavelength of maximum absorbance (λ_{max}) and the molar absorption coefficient at λ_{max} measured here are in good agreement with values reported by Falk et al. (1989). Domoic acid absorbance is considerably lower at longer wavelengths ($>290 \text{ nm}$). The molar absorption coefficient of domoic acid varies from 17.7 to $29.9 \text{ L mol}^{-1} \text{ cm}^{-1}$ in the UV-B range (280–320 nm) and from 2.8 to $17.7 \text{ L mol}^{-1} \text{ cm}^{-1}$ in the UV-A range (320–400 nm). This result indicates that domoic acid still directly absorbs radiation in the wavelength range relevant to environmental photochemical processes ($>290 \text{ nm}$). Molar absorption coefficients in the UV-B and UV-A wavelength range have been previously presented by Falk et al. (1989). However, these authors measured domoic acid absorbance only at low concentration ($\sim 16 \mu\text{mol L}^{-1}$) and reported values at wavelengths longer than $\sim 275 \text{ nm}$ that are too low to make comparison with our results possible. The strong absorption bands centered at 242 nm have been attributed to the π, π^* electronic transition of the conjugated double bond (Wu et al. 2000).

Photodegradation of domoic acid in seawater—A series of six controlled photodegradation experiments were conducted to determine the rate of domoic acid photodegradation in natural waters under simulated sunlight. Each experiment consisted of the addition of domoic acid to $0.2 \mu\text{m}$ -filtered WBSW. Duplicate light-exposed and dark control samples were taken every 2 h. All samples were derivatized with FMOC-Cl and analyzed by HPLC. A representative plot of the change of domoic acid concentrations as a function of irradiation time is presented in Fig. 3. There was a significant loss of domoic acid over the 10-h incubation period in light-exposed cells, with concentrations decreasing exponentially as a function of irradiation time from, on average, 84 to 18 nmol L^{-1} (Fig. 3). This result is similar to the results obtained in a preliminary study by Bates et al. (2003), who found approximately 75% of an added domoic acid spike was degraded after a 22-h exposure to full-spectrum simulated sunlight in seawater. No loss of domoic acid was observed in dark controls (Fig. 3), indicating that light was responsible for the loss of domoic acid in these samples. The photoproduction of three photoproducts of domoic acid

has been observed in all experiments. The photochemistry of these photoproducts will be discussed in detail in a related manuscript (Bouillon et al. unpubl. data).

Observed first-order rate coefficients of domoic acid degradation in the WBSW samples, k_{obs} , were obtained by linear regression of the logarithmic-transformed domoic acid concentrations versus irradiation time (Table 1, WBSW). Resulting k_{obs} values were normalized to an average irradiance of 7.8 mW cm^{-2} (integrated over 280–400 nm), which is 1.2 times midday natural sunlight measured at 34°N in mid-July. The corresponding average first-order rate coefficient of domoic acid degradation in these six WBSW samples was $0.15 \pm 0.01 \text{ h}^{-1}$ ($n = 6$).

Role of environmental factors on the kinetics of domoic acid photodegradation—A second series of controlled photodegradation experiments was conducted to determine the influence of the sample matrix on the rate of domoic acid photodegradation in seawater. In the first of these experiments, seawater was replaced with DIW prior to photodegradation of the added domoic acid. The resulting k_{obs} measured for the photochemical loss of domoic acid in DIW was 0.16 h^{-1} , which is statistically equivalent (t -test, 95% confidence level) to the first-order rate coefficient in WBSW. These results indicate that ambient components of the WBSW matrix do not impact the photochemical degradation rate of domoic acid and indicate that the toxin undergoes direct photochemical degradation in seawater. In a preliminary study with somewhat higher concentrations, Bates et al. (2003) also observed that the photochemical loss of domoic acid in solutions prepared with deionized water, artificial seawater, and natural seawater were essentially the same.

In a second experiment exploring the role of the sample matrix on domoic acid photodegradation, photochemically labile extracted humic materials ($\sim 20 \text{ mg L}^{-1}$) were added to the DIW prior to photodegradation. The value of k_{obs} was corrected for light screening by chromophoric dissolved organic matter (CDOM) (Schwarzenbach et al. 1993). There was again no significant difference (t -test, 95% confidence level) in the k_{obs} values obtained with and without added humic materials (Table 1), indicating that the photodegradation of domoic acid is not induced by added humic materials. Results from this study indicate that indirect or sensitized photochemical processes do not play an important role in the photodegradation of domoic acid in seawater.

The apparent absence of a sensitized pathway in the photodegradation of domoic acid in seawater or DIW spiked with humic materials is somewhat surprising. Compounds containing conjugated double-bond moieties are generally good triplet energy acceptors (Turro 1978). In natural waters, absorption of solar radiation by CDOM initially results in the formation of a singlet excited species ($^1\text{CDOM}^*$), which decays, in part, by undergoing intersystem crossing to excited triplet excited state CDOM ($^3\text{CDOM}^*$). Reactions between a triplet state species and compounds containing an ethylene or polyene moiety often result in isomerization of the double bond (Turro 1978). Photosensitized isomerization of compounds containing conjugated double-bond moieties is known to occur in natural waters. For example, Zepp et

al. (1985) employed the photoisomerization of 1,3-pentadiene to investigate the nature and occurrence of the excited triplet state generated upon irradiation of dissolved organic matter in natural waters. In addition, photoisomerization of the diene moiety of the algal toxin microcystins has also been observed (Tsuji et al. 1994; Welker and Steinberg 2000). These authors observed that microcystins are stable in deionized water when exposed to natural sunlight. However, Tsuji et al. (1994) demonstrated that microcystins were photoisomerized when extracted algal pigments, serving as photosensitizers, were added to irradiation solutions. Direct comparison of the results presented in Table 1 and results of these earlier studies should be viewed carefully, however, as Tsuji et al. (1994) conducted their photochemical experiments using a very high concentration of sensitizer, and Zepp et al. (1985) employed high concentrations of 1,3-pentadiene.

To evaluate the role of oxygen in the photodegradation of domoic acid, a solution of WBSW was purged with N_2 for 4 h prior to irradiation in order to significantly reduce the concentration of dissolved O_2 . The resulting k_{obs} (0.15 h^{-1}) in this N_2 -purged sample was statistically equivalent (t -test, 95% confidence level) to the first-order rate coefficient in the air-saturated WBSW (Table 1). This indicates that the decrease in the excited triplet state quencher dissolved oxygen did not influence the rate of photodegradation of domoic acid. These results indicate that sensitized photodegradation is not an important removal process for domoic acid in WBSW, a result that is in agreement with the results obtained with the addition of humic material to DIW. Results from this study do not, however, entirely exclude the presence of sensitized pathways in the photochemical transformation of domoic acid, but rather indicate that sensitized pathways are considerably slower or much less energetically efficient relative to the direct photochemical pathway.

The role of trace metals on the photochemical degradation rate of domoic acid was also investigated. A recent study by Rue and Bruland (2001) demonstrated that domoic acid is an effective chelator for Cu(II) and Fe(III). This is not completely unexpected, since the carboxyl groups in domoic acid chelate such metal cations. The occurrence of chelated domoic acid complexes may be very significant to the ultimate fate of the dissolved fraction of the toxin in seawater, because the photoreactivity of organic matter is often enhanced when bound to trace metals such as Fe and Cu (Sykora 1997; Barbeau et al. 2001). Several Fe(III)-ligand and Cu(II)-ligand complexes undergo photodegradation in natural sunlight, resulting in partial ligand breakdown and changes in iron and copper speciation (Sykora 1997; Voelker et al. 2000; Barbeau et al. 2001). These results lead us to hypothesize that the demonstrated complexation of domoic acid by redox-active trace metals such as Cu(II) and Fe(III) may influence the efficiency of the photodegradation process.

Addition of 100 nmol L^{-1} Cu(II) and 107 nmol L^{-1} Fe(III) separately to WBSW did not, however, significantly affect the k_{obs} (Table 1: WBSW + Cu; WBSW + Fe) relative to WBSW samples with no added metals (t -test, 95% confidence level). There are several possibilities that may explain this result: (1) complexation of domoic acid with either Fe or Cu does not influence its photochemical degradation; (2)

ambient organic ligands in the WBSW complexed most of the added Fe and Cu, leaving domoic acid uncomplexed; (3) the pH of the irradiation solution influenced the photoreactivity of the Fe(III)–domoic acid complex; or (4) inorganic constituents of seawater inhibited the phototransformation of the Fe(III)–domoic acid complex.

In coastal seawater, typical concentrations of total dissolved Fe and strong Fe(III)-complexing ligands are 0.5–10 nmol L⁻¹ and 1.5–12 nmol L⁻¹, respectively, with ligands usually in a significant excess compared to dissolved Fe (Boye et al. 2003; Powell and Wilson-Finelli 2003). Similarly, in the coastal waters of southeastern North Carolina, concentrations of strong Cu-complexing ligands (4–126 nmol L⁻¹) are in excess of total dissolved Cu (2.1–9.3 nmol L⁻¹) (Shank et al. 2004a). In our experiments utilizing ambient metal levels, speciation calculations using the conditional stability constants for Fe(III)– and Cu(II)–domoic acid complexes in seawater reported by Rue and Bruland (2001) indicate that strong naturally occurring ligands should be the dominant chelators of Fe(III) and Cu(II). In the metal-addition experiments, it is likely that the added Fe(III) and Cu(II) at the concentrations of ≥ 100 nmol L⁻¹ titrated the naturally occurring strong ligands, leaving the excess metal to complex weaker natural ligands and domoic acid. Without detailed speciation studies for Fe(III) and Cu(II) in these samples, we cannot evaluate exactly how important domoic acid would be as a chelator in these experiments.

In order to explore these possibilities, a separate series of photochemical experiments was conducted. In the first experiment, 100 nmol L⁻¹ Fe(III) was added to a solution of domoic acid prepared in DIW followed by irradiation. Addition of Fe(III) to DIW resulted in a dramatic increase in the k_{obs} value (0.26 h⁻¹) relative to deionized water without Fe(III) (Table 1: DIW + Fe). This is consistent with results reported by Bates et al. (2003), who also found that domoic acid in the presence of Fe(III) was almost completely degraded in deionized water, but only 36% degraded in deionized water without added Fe(III). Both studies demonstrate that in deionized water, the photoreactivity of domoic acid is greatly enhanced in the presence of Fe(III).

Another experiment was conducted using a UV-irradiated, trace-metal clean seawater sample. The sample was UV-irradiated by a 1.2-kW high-pressure Hg vapor lamp (Ace Glass) for 6 h to remineralize the dissolved organic matter present in the sample. Dissolved organic carbon analysis performed before and after UV irradiation indicated that all organics were photo-oxidized by this process. Trace metals were removed by passing the seawater sample through a Chelex-100 (Biorad) column. However, removal of the ambient trace metals and organics had no impact on k_{obs} , indicating that neither parameter influenced the photochemical degradation rate coefficient of domoic acid in seawater.

A series of experiments was also conducted to determine the effect of pH on the photodegradation of domoic acid in WBSW spiked with 107 nmol L⁻¹ Fe(III). The pH of the irradiation solutions was adjusted to 4, 5, 6, or 7 by adding HCl. Results (Table 1) indicate that changes in the pH of the irradiation solution did not affect the rate of photodegradation of domoic acid in seawater. An additional pH experiment was conducted in which the pH of WBSW was ad-

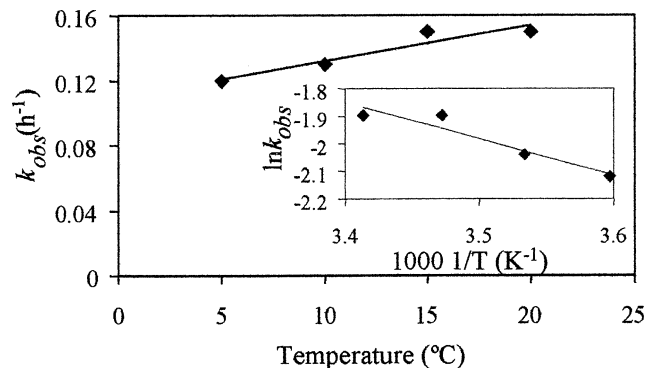


Fig. 4. Temperature dependence of the observed first-order rate coefficients domoic acid photodegradation (k_{obs}). The inset Arrhenius plots are the natural log of k_{obs} versus 1,000 divided by temperature in Kelvin.

justed to pH ~ 4 prior to the addition of domoic acid and Fe(III) (data not shown). This procedure took into consideration the formation of colloidal suspensions that may occur with the addition of Fe(III) to the irradiation solution. Nevertheless, addition of domoic acid and Fe(III) after pH adjustment did not alter the rate of photodegradation, thus indicating that the order of reagent addition was not important.

The reasons for which Fe(III) addition considerably increased the photochemical degradation rate of domoic acid in deionized water and not in seawater are not entirely clear. One possibility is that iron photo-redox reactions in aqueous solution produce reactive oxygen species such as hydroxyl radical, which may react with domoic acid. In seawater, scavenging by inorganic species such as bromide and bicarbonate/carbonate anions consumes most of the hydroxyl radical production, making them unavailable for degradation of domoic acid (Mopper and Zhou 1990). Also, as pointed out by Bates et al. (2003), the chemical speciation of Fe(III) is very different in deionized water compared with seawater; therefore, photochemical mechanisms would differ as well.

Temperature dependence—Domoic acid has been detected in a variety of coastal seawater locations of varying temperature regimes, such as Prince Edward Island, the Washington State Coast, and Monterey Bay (Bates et al. 1989; Trainer et al. 2000, 2002). In order to determine the effect of temperature on the rate of domoic acid photodegradation, experiments were performed at 5°C, 10°C, 15°C, and 20°C. The photodegradation rate coefficients of domoic acid increased from 0.12 h⁻¹ at 5°C to 0.15 h⁻¹ at 20°C (Fig. 4). The activation energy for the photodegradation of domoic acid was determined from the Arrhenius equation:

$$\ln k_{\text{obs}} = \ln A - \frac{E_a}{RT} \quad (4)$$

where T is the temperature (Kelvin), R is the general gas constant (8.314 J mol⁻¹ K⁻¹), E_a is the activation energy, and A is the frequency factor. The temperature dependence of the photodegradation of domoic acid is characterized by an activation energy of 13 kJ mol⁻¹. The observed increase of the rate of domoic acid photodegradation with temperature indicates that this environmental factor must be taken

Table 3. Daily integrated surface ultraviolet radiation (UV: 280–400 nm), modeled seawater attenuation coefficient at 330 nm [K_d (330 nm)], and modeled turnover rate constants for domoic acid photodegradation k_{DA} (d^{-1}) for each location.*

Location	UV (280–400) ($\text{kJ m}^{-2} \text{d}^{-1}$)	K_d (330 nm) (m^{-1})	k_{DA} (d^{-1})
Prince Edward Island	887	5.4	0.017
Washington State Coast	822	2.3	0.019
Monterey Bay, California	1,170	1.6	0.035

into account in estimation of the photochemical loss rates of domoic acid in natural waters.

Quantum yield determination—The wavelength dependence of the quantum yield for domoic acid photodegradation was determined using monochromatic irradiation rather than full-spectrum simulated sunlight. To our knowledge, this is the first study to report the quantum yield for the photochemical degradation of an algal toxin. Since it appears that domoic acid undergoes direct photochemical degradation, the quantum yield for the photodegradation of domoic acid [$\Phi_{DA}(\lambda)$] in an optically thin solution is given by the following expression (Zepp 1978):

$$\Phi_{DA}(\lambda) = \frac{-\ln[DA]_t/[DA]_o(\lambda)/t}{2.303E_o(\lambda)(A/V)\varepsilon(\lambda)} \quad (5)$$

where $-\ln[DA]_t/[DA]_o(\lambda)/t$ is the wavelength-dependent first-order rate coefficient for domoic acid (DA) photodegradation, $E_o(\lambda)$ (mol photons $\text{m}^{-2} \text{s}^{-1}$) is the irradiance, A is exposed area (m^2), V is the volume of the irradiated cell (m^3), $\varepsilon(\lambda)$ ($\text{L mol}^{-1} \text{cm}^{-1}$) is the molar absorption coefficient of domoic acid, and l (cm) is the radiation path length in the irradiated cell.

The wavelength dependence of the quantum yields for the photodegradation of domoic acid determined in DIW and WBSW from 280 to 404.5 nm at $23^\circ\text{C} \pm 1^\circ\text{C}$ are presented in Table 2. The $\Phi_{DA}(\lambda)$ values determined in WBSW were corrected for irradiation screening by CDOM not present in DIW (Schwarzenbach et al. 1993). Quantum yields for domoic acid photodegradation varied from 0.032 to 0.20 in the UV wavelength range in both seawater and DIW solutions. For both solutions, no photochemical loss of domoic acid was detected at 404.5 nm. As is the case with many other marine photochemical reactions, radiation in the UV-B (280–320 nm) is most effective at inducing domoic acid photochemical degradation, whereas visible light has no apparent effect. Quantum yields for domoic acid photodegradation in both WBSW and DIW solutions showed the same wavelength dependence. This was expected, since we found that k_{obs} values determined in DIW and in WBSW were not significantly different. Quantum yields for domoic acid photodegradation found in this study are relatively high compared to other direct marine photochemical reactions, such as hydroxyl radical production from nitrate and nitrite photolysis (Jankowski et al. 1999). As a consequence, even if domoic acid weakly absorbs in the solar radiation range (Fig. 2), it is readily photodegraded because of its high quantum yields.

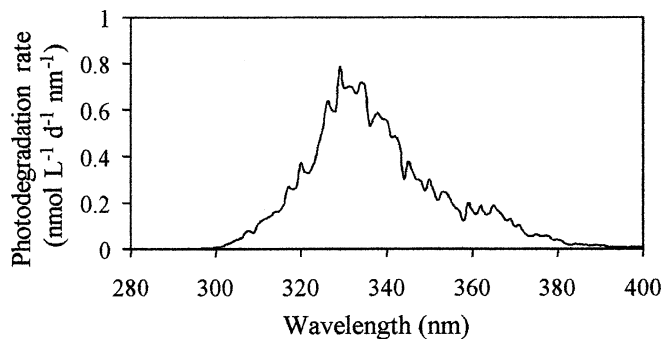


Fig. 5. Representative plot of the modeled photodegradation rate of domoic acid just below the surface plotted as a function of wavelength for a concentration of 100 nmol L^{-1} domoic acid at Monterey Bay (MB).

Estimation of in situ photodegradation of domoic acid—In this study, the potential in situ rates and turnover rate constants for the photodegradation of domoic acid have been estimated for various coastal locations using determined quantum yields and modeled solar irradiance and attenuation coefficient values for early-fall cloudless days. To our knowledge, this is the first time that the in situ photochemical degradation of a marine algal toxin has been modeled. The photochemical degradation rate for any direct photochemical process depends on the molar absorption coefficient of the compound, the quantum yields of the reaction, and on highly variable local conditions such as solar irradiance, water optical properties, and water temperature (Zafiriou et al. 1984). Values of $\Phi_{DA}(\lambda)$ for the undetermined wavelengths have been approximated by linear interpolation of the $\Phi_{DA}(\lambda)$ measured in this study. Since there is no available data set on the vertical distribution of dissolved domoic acid in natural waters, calculations in this section were made by assuming that the concentration of domoic acid (100 nmol L^{-1}) was uniform throughout the interval depth considered. The wavelength dependence of the photodegradation rates of domoic acid, $P_{DA}(\lambda, 0-)$ ($\text{nmol L}^{-1} \text{d}^{-1} \text{nm}^{-1}$), just below the water surface was calculated using the following expression using modeled solar irradiance [$E_o(\lambda, 0-)$]:

$$P_{DA}(\lambda, 0-) = 2.303[DA]E_o(\lambda, 0-)\Phi_{DA}(\lambda)\varepsilon(\lambda) \quad (6)$$

Calculated photochemical loss rates of domoic acid were higher at Monterey Bay, since higher values of solar irradiance (see Table 3) have been estimated for this location. As illustrated in Fig. 5, the results clearly demonstrate that domoic acid photodegradation is initiated mainly by UV solar radiation, primarily at wavelengths between 315 and 355 nm, with maximum photodegradation observed at about 330 nm. We calculated that UV-B potentially accounted for more than 9% and UV-A for more than 90% of the total domoic acid photodegradation near the sea surface. These results are expected, since values of $\Phi_{DA}(\lambda)$ have been found to tail down to zero in the visible wavelength range (Table 2). Photodegradation rates of domoic acid as a function of depth $P_{DA}(\lambda, z)$ ($\text{mol L}^{-1} \text{d}^{-1}$) were computed using Eq. 7:

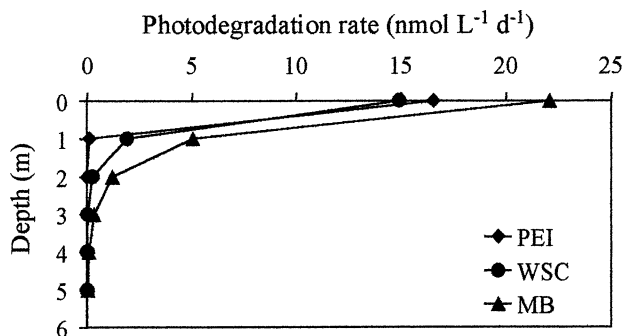


Fig. 6. Modeled photodegradation rate of domoic acid as a function of depth for a concentration of 100 nmol L^{-1} domoic acid at Prince Edward Island (PEI), Washington State Coast (WSC), and Monterey Bay (MB).

$$P_{\text{DA}}(\lambda, z) = \int_{280}^{400} P_{\text{DA}}(\lambda, 0-) e^{-K_d(\lambda)z} d\lambda \quad (7)$$

where $K_d(\lambda)$ is the spectral attenuation coefficients value estimated from remote sensing (SeaWiFS) measurements using the algorithm SeaUV. Values of $K_d(\lambda)$ calculated at 330 nm for each location are presented in Table 3. Values of $P_{\text{DA}}(\lambda, z)$ were computed at every 1-m interval down to 5 m in depth for the three different locations (Fig. 6). Higher values were observed near the surface, where solar irradiance is highest, and rates decrease rapidly with depth (Fig. 6). Domoic acid photodegradation was limited to the upper few meters or centimeters of the water column. We calculated that $P_{\text{DA}}(\lambda, z)$ values fall to 1% of its surface values at 0.8, 2.3, and 3.4 m for Prince Edward Island, Washington State Coast, and Monterey Bay locations, respectively. The more rapid decrease of $P_{\text{DA}}(\lambda, z)$ with depth observed at Prince Edward Island is directly related to the high $K_d(\lambda)$ values estimated for this location. In contrast to Washington State Coast and Monterey Bay, which are located at a distance greater than 10 km away from the coast, Prince Edward Island is an inshore location highly influenced by terrestrial input of dissolved and particulate organic and inorganic matter that influence $K_d(\lambda)$.

The turnover rate constants k_{DA} (d^{-1}) were obtained by dividing the vertically integrated (0–5-m) daily photochemical loss of domoic acid $\int_0^5 P_{\text{DA}}(\lambda, z) dz$ (moles DA $\text{m}^{-2} \text{d}^{-1}$) by the concentration of domoic acid integrated over the depth interval considered $[\text{DA}]_{0-5}$ (moles DA m^{-2}):

$$k_{\text{DA}} = \frac{\int_0^5 P_{\text{DA}}(\lambda, z) dz}{[\text{DA}]_{0-5}} \quad (8)$$

Calculated k_{DA} values ranged from 0.017 to 0.035 d^{-1} for the locations considered (Table 3). Therefore, from 1.7% to 3.5% of the standing dissolved domoic acid concentration in the top 5 m of the water column was photochemically removed on a daily basis. The purpose of this modeling exercise was an initial attempt to evaluate the relative importance of photochemical reaction as a sink for dissolved domoic acid in natural waters. Further work using in situ measurements in bloom conditions of the solar irradiance

intensity, the spectral attenuation coefficient of the water column, and dissolved domoic acid concentrations are needed to achieve more realistic calculations of the rate of photodegradation of domoic acid.

The findings of our study are noteworthy from several points of view. First, we have shown that domoic acid is most likely photodegraded via a direct photochemical pathway. Thus, the molar absorption coefficient and quantum yield of domoic acid reported in this article can be used to predict the photochemical loss rate of this compound for other locations and times of the year. Second, we have demonstrated that photodegradation is an environmentally important sink for dissolved domoic acid, since it is degraded by sunlight in seawater on a time scale of days. However, in order to assess whether photochemical removal is a dominant sink for dissolved domoic acid, other sinks, such as bacterial consumption, adsorption to particles, and dilution, need to be quantified in field conditions.

References

- BARBEAU, K., E. L. RUE, K. W. BRULAND, AND A. BUTLER. 2001. Photochemical cycling of iron in the surface ocean mediated by microbial iron(III) binding ligands. *Nature* **413**: 409–413.
- BATES, S. S., C. LÉGER, M. L. WELLS, AND K. HARDY. 2003. Photodegradation of domoic acid. p. 30–35. *In* S. S. Bates [ed.], *Proceedings of the Eighth Canadian Workshop on Harmful Marine Algae*. **2498**.
- , AND OTHERS. 1989. Pennate diatom *Nitzschia pungens* as the primary source of domoic acid, a toxin in shellfish from eastern Prince Edward Island, Canada. *Can. J. Fish. Aquat. Sci.* **46**: 1203–1215.
- BOYE, M., A. P. ALDRICH, C. M. G. VAN DEN BERG, J. T. M. DE JONG, M. VELDHIJS, AND H. J. W. DE BAAR. 2003. Horizontal gradient of the chemical speciation of iron in surface waters of the northeast Atlantic Ocean. *Mar. Chem.* **80**: 129–143.
- CULLEN, J. J., R. F. DAVIS, J. S. BARTLETT, AND W. L. MILLER. 1997. Toward remote sensing of UV attenuation, photochemical fluxes and biological effects in surface waters, p. 97. *In* *Proceedings of the 1997 Aquatic Sciences Meeting*. ASLO.
- DOUCETTE, G. J., C. A. SCHOLIN, J. P. RYAN, J. V. TYRRELL, R. MARIN, AND C. L. POWELL. 2002. Possible influence of *Pseudo-nitzschia australis* population and toxin dynamics on food web impacts in Monterey Bay CA USA. 10th Harmful Algal Bloom Conference, St. Pete, Florida, 21–25 October 2002.
- FALK, M., J. A. WALTER, AND P. W. WISEMAN. 1989. Ultraviolet spectrum of domoic acid. *Can. J. Chem.* **67**: 1421–1425.
- FICHOT, C. G. 2004. Marine photochemistry from space. M.Sc. thesis, Dalhousie Univ.
- GORDON, H. R. 1989. Can the Lambert-Beer law be applied to the diffuse attenuation coefficient of ocean water? *Limnol. Oceanogr.* **34**: 1389–1409.
- HAMMOND, G. S., AND OTHERS. 1964. Mechanisms of photochemical reaction in solution. XXII. Photochemical *cis-trans* isomerization. *J. Am. Chem. Soc.* **86**: 3197–3217.
- HAMPSON, D. R., X. P. HUANG, J. W. WELLS, J. A. WALTER, AND J. L. WRIGHT. 1992. Interaction of domoic acid and several derivatives with kainic acid and AMPA binding sites in rat brain. *Eur. J. Pharmacol.* **218**: 1–8.
- HATCHARD, C. G., AND C. A. PARKER. 1956. A new sensitive chemical actinometer. II. Potassium ferrioxalate as a standard chemical actinometer. *Proc. R. Soc.* **235A**: 518–536.
- HORNER, R. A., D. L. GARRISON, AND F. G. PLUMLEY. 1997. Harm-

- ful algal blooms and red tide problems on the U.S. west coast. *Limnol. Oceanogr.* **42**: 1076–1088.
- JANKOWSKI, J. J., D. J. KIEBER, AND K. MOPPER. 1999. Nitrate and nitrite ultraviolet actinometers. *Photochem. Photobiol.* **70**: 319–328.
- JERLOV, N. G. 1976. *Marine optics*. Elsevier Scientific.
- KIRK, J. T. O. 1994. *Light and photosynthesis in aquatic systems*, 2nd ed. Cambridge Univ. Press.
- LEFEBVRE, K. A., S. BARGU, T. KIECKHEFER, AND M. W. SILVER. 2002. From sanddabs to blue whales: The pervasiveness of domoic acid. *Toxicol.* **40**: 971–977.
- LEMAIRE, J., I. CAMPBELL, H. HULPKE, J. A. GUTH, W. MERZ, J. PHILP, AND C. VON WALDOW. 1982. An assessment of test methods for photodegradation of chemicals in the environment. *Chemosphere* **11**: 119–164.
- MADRONICH, S., AND S. FLOCKE. 1998. *The role of solar radiation in atmospheric chemistry*. Springer-Verlag.
- MALDONADO, M. T., M. P. HUGHES, E. L. RUE, AND M. L. WELLS. 2002. The effect of Fe and Cu on growth and domoic acid production *Pseudo-nitzschia multiseriata* and *Pseudo-nitzschia australis*. *Limnol. Oceanogr.* **47**: 515–526.
- MOPPER, K., AND X. ZHOU. 1990. Hydroxyl radical photoproduction in the sea and its potential impact on marine processes. *Science* **250**: 661–664.
- POCKLINGTON, R., J. E. MILLEY, S. S. BATES, C. J. BIRD, A. S. W. DE FREITAS, AND M. A. QUILLIAM. 1990. Trace determination of domoic acid in seawater and phytoplankton by high-performance liquid chromatography of the fluorenylmethoxycarbonyl (Fmoc) derivative. *Intern. J. Environ. Anal. Chem.* **38**: 351–368.
- POWELL, R. T., AND A. WILSON-FINELLI. 2003. Importance of organic Fe complexing ligands in the Mississippi River plume. *Estuar. Coastal Shelf Sci.* **38**: 351–368.
- RUE, E., AND K. BRULAND. 2001. Domoic acid binds iron and copper: A possible role for the toxin produced by the marine diatom *Pseudo-nitzschia*. *Mar. Chem.* **76**: 127–134.
- SCHOLIN, C. A., AND OTHERS. 2000. Mortality of sea lions along the central California coast linked to a toxic diatom bloom. *Nature* **403**: 80–84.
- SCHWARZENBACH, R. P., P. M. GSCHWEND, AND D. M. IMBODEN. 1993. *Environmental organic chemistry*. Wiley-Interscience.
- SHANK, G. C., S. A. SKRABAL, R. F. WHITEHEAD, G. B. AVERY, AND R. J. KIEBER. 2004b. River discharge of strong Cu-complexing ligands to South Atlantic Bight waters. *Mar. Chem.* **88**: 41–51.
- , ———, AND R. J. KIEBER. 2004a. Strong copper complexation in an organic estuary: The importance of allochthonous dissolved organic matter. *Mar. Chem.* **88**: 21–39.
- STEWART, J. E., L. J. MARKS, M. W. GILGAN, E. PFEIFFER, AND B. M. ZWICKER. 1998. Microbial utilization of the neurotoxin domoic acid: Blue mussels (*Mytilus edulis*) and soft shell clams (*Mya arenaria*) as sources of the microorganisms. *Can. J. Microbiol.* **44**: 456–464.
- SYKORA, J. 1997. Photochemistry of copper complexes and their environmental aspects. *Coord. Chem. Rev.* **159**: 95–108.
- TODD, E. C. D. 1993. Amnesic shellfish poisoning—a review. *J. Food Protection* **56**: 69–83.
- TRAINER, V. L., B. M. HICKEY, AND R. A. HORNER. 2002. Biological and physical dynamics of domoic acid production off the Washington coast. *Limnol. Oceanogr.* **47**: 1438–1446.
- , AND OTHERS. 2000. Domoic acid production near California coastal upwelling zones, June 1998. *Limnol. Oceanogr.* **45**: 1818–1833.
- TSUJI, K., S. NAITO, F. KONDO, N. ISHIKAWA, M. F. WATANABE, M. SUZUKI, AND K. HARADA. 1994. Stability of microcystins from cyanobacteria: Effect of light on decomposition and isomerization. *Environ. Sci. Technol.* **28**: 173–177.
- TURRO, N. J. 1978. *Modern molecular photochemistry*. The Benjamin/Cumming Publishing Company.
- VOELKER, B. M., D. L. SEDLAK, AND O. C. ZAFIRIOU. 2000. Chemistry of superoxide radical in seawater: Reactions with organic Cu complexes. *Environ. Sci. Technol.* **34**: 1036–1042.
- WELKER, M., AND C. STEINBERG. 2000. Rates of humic substance photosensitized degradation of microcystin-LR in natural waters. *Environ. Sci. Technol.* **34**: 3415–3419.
- WRIGHT, J. L. C., M. FALK, A. G. MCINNES, AND J. A. WALTER. 1990. Identification of isodomoic acid D and two new geometrical isomers of domoic acid in toxic mussels. *Can. J. Chem.* **68**: 22–25.
- , AND M. A. QUILLIAM. 1995. Methods for domoic acid, the amnesic shellfish poisons, p. 113–133. *In* G. M. Hallegraeff, D. M. Anderson, and A. D. Cembella [eds.], *IOC manual on harmful marine algae*, IOC manuals and guides 33. UNESCO.
- , AND OTHERS. 1989. Identification of domoic acid, a neuroexcitatory amino acid, in toxic mussels from eastern Prince Edward Island. *Can. J. Chem.* **67**: 481–490.
- WU, G., AND OTHERS. 2000. UV resonance raman detection and quantification of domoic acid in phytoplankton. **72**: 1666–1671.
- ZAFIRIOU, O. C., J. JOUSSOT-DUBIEN, R. G. ZEPP, AND R. G. ZIKA. 1984. Photochemistry of natural waters. *Environ. Sci. Technol.* **18**: 358A–371A.
- ZAR, J. H. 1984. *Biostatistical analysis*, 2nd ed. Prentice-Hall.
- ZEPP, R. G. 1978. Quantum yields for reaction of pollutants in dilute aqueous solution. *Environ. Sci. Technol.* **12**: 327–329.
- , AND D. M. CLINE. 1977. Rates of direct photolysis in aquatic environment. *Environ. Sci. Technol.* **11**: 359–366.
- , P. F. SCHLOTZHAUER, AND R. M. SINK. 1985. Photosensitized transformations involving electronic energy transfer in natural waters: Role of humic substances. *Environ. Sci. Technol.* **19**: 74–81.

Received: 7 March 2005

Accepted: 24 August 2005

Amended: 21 September 2005